Applied Mathematical Modelling 39 (2015) 5598–5615

Contents lists available at ScienceDirect

Applied Mathematical Modelling

journal homepage: www.elsevier.com/locate/apm

Five-unknowns generalized hybrid-type quasi-3D HSDT for advanced composite plates

J.L. Mantari [a,b], C. Guedes Soares [a,*]

[a] Centre for Marine Technology and Engineering (CENTEC), Instituto Superior Técnico, Universidade de Lisboa, Av. Rovisco Pais, 1049-001 Lisbon, Portugal
[b] Presently at Universidad de Ingeniería y Tecnología, Av. Cascanueces 2221, Santa Anita, Lima, Peru

ARTICLE INFO

Article history:
Received 24 May 2013
Received in revised form 7 December 2014
Accepted 12 January 2015
Available online 22 January 2015

Keywords:
Higher order shear deformation theory
Bending analysis
Functionally graded materials
Trigonometric plate theory
Stretching effect

ABSTRACT

In this paper a 5-unknowns generalized hybrid-type quasi-3D HSDT for the static analysis of functionally graded single and sandwich plates is presented. Generalized hybrid-type modeling can adopted with any kind of shear strain shape functions for the inplane and transverse displacement, and therefore infinite hybrid-type (non-polynomial, polynomial, mixed type) displacement based shear deformation theory complying with the free surface boundary condition can be obtained. The key feature of this theory is that, in addition to including stretching, it has only 5 unknowns in the displacement field modeling as the first order shear deformation theory (FSDT). The generalized hybrid-type theory is also quasi-3D because the 3D Hooke's law equation is utilized, i.e. $\sigma_{zz} \neq 0$. The generalized governing equations and boundary conditions are derived by employing the principle of virtual works. A generalized Navier-type closed-form solution is obtained for functionally graded single and sandwich plates subjected to transverse load for simply supported boundary conditions. Analytical results from the new generalized hybrid-type quasi-3D higher order shear deformation theory (HSDT) are compared with the FSDT, other quasi-3D HSDTs, and refined HSDTs. The fundamental conclusions that emerge from the present numerical results suggest that: (a) infinite shears strain shape function can be evaluated by using the present theory; (b) polynomial shear strain functions appear to be a good choice for the implementing of a quasi-3D HSDT based on this generalized quasi-3D hybrid type HSDT; (c) this generalized theory can be as accurate as the 6-unknown generalized hybrid-type quasi-3D HSDT; (d) the *best HSDT* with stretching effect and 5-unknows can be obtained from the present generalized theory, this can be done by optimizing a theory that for example has a given non-polynomial inplane and transverse shears strain shape functions.

© 2015 Elsevier Inc. All rights reserved.

1. Introduction

Functionally graded materials (FGMs) have engineered gradients of composition, structure and/or specific properties in preferred directions. FGMs have superior mechanical response for certain applications than homogeneous material composed of similar constituents. The mechanical properties vary smoothly and continuously in preferred directions in FGMs such as functionally graded plates (FGPs).

* Corresponding author. Tel.: +351 218417957.
E-mail address: c.guedes.soares@centec.tecnico.ulisboa.pt (C. Guedes Soares).

http://dx.doi.org/10.1016/j.apm.2015.01.020
0307-904X/© 2015 Elsevier Inc. All rights reserved.

Although the concept of FGMs is not new [1,2], and fabrication of FGMs is still a topic of research, it is interesting to see such advanced materials and their complexity in the nature (sea shells, bones, etc.). Several areas of application for FGMs guarantee that this kind of material will be more and more demanding in a near future. An extended literature review on FGMs can be found in Refs. [3–9]. In what follows, in order to complete the review of the contributions on the analytical modeling of FGPs, interesting research works contributions conducted during this decade is described.

Carrera et al. [10] investigated the influence of the stretching effect on the static responses of FGPs and shells. Neves et al. [11,12] and Ferreira et al. [13] developed a quasi-3D hybrid type (polynomial and trigonometric) HSDT for the static and free vibration analysis of FGPs by using both meshless numerical method, and the Carreras's Unified Formulation (CUF). The development of *meshless-CUF* as well as the *best plate theory diagram* based on CUF [14–19] (which can be called the second generation of the shear deformation theories) are both very interesting research works with remarkable contribution to the literature. Interestingly, in Refs. [11–13], the new introduced displacement fields use different non-polynomial shear strain shape functions for in-plane displacements, and a polynomial one for the out-of-plane displacement. Moreover, Refs. [20–25] introduced several new non-polynomial shear strain shape functions, which were found to be important to solve classical and advanced composite problems due to the achievement of accuracy in bending results. Refs. [4–8] present bending results of FGPs by using new non-polynomial HSDTs. In Refs. [6,7], the stretching effect in non-polynomial quqasi-3D HSDTs was studied. There appear actual demand for new non-polynomial shear strain shape functions, and in this paper, some new ones are provided for the first time.

Based on the interesting work on the 2-unknows plate theory for isotropic and orthotropic plates [26–28], Mechab et al. [29] investigated the bending behavior of FGPs by using 4-unknowns HSDT with polynomial shear strain shape function. Abdelaziz et al. [30] evaluated the static analysis of FGPs with the same HSDT. Houari et al. [31] and Hamidi et al. [32] analyzed the thermoelastic behavior of FGPs by the 4-unknows HSDT with polynomial shear strain shape function. Consequently, Mechab et al. [33] investigated the static and dynamic analysis of FGPs with new non-polynomial HSDT (hyperbolic shear strain shape function). Recently, a 5-unknowns trigonometric plate theory (TPT) with thickness stretching effect was developed by Thai and Kim [34] with good accuracy respect its counterpart the 6-unknows TPT. Based on this work, the authors [35] developed an optimized TPT with thickness stretching effect and 5-unknowns with improved results.

Review on generalized formulations of shear deformation theories [25,36–40] for classical and advanced composites reveals that no much work on the topic is found. Moreover, generalized formulations for advanced composites [10,41–44] are even less. In Ref. [7], a generalized quasi-3D hybrid type HSDT for FGPs was developed. The interesting feature of this generalized theory is its capability to reproduce the HSDTs described above with the exception of the ones formulated by Carrera [10].

The key feature of the present quasi-3D HSDTs are both the reduced number of unknowns and the thickness expansion modeling ($g(z)$). Normally, this shear strain shape function is conditioned by the in-plane displacement model ($f(z)$), i.e. ($g(z) = f'(z)$). As a result, there is no freedom in selecting an arbitrary through the thickness displacement field. The present formulation has that freedom, i.e. ($g(z) \neq f'(z)$), and therefore, infinite hybrid type quasi-3D shear deformation theories with stretching effect (polynomial or non-polynomial or hybrid type) can be created just having 5 unknowns. The present generalized quasi-3D hybrid type HSDT for FGPs as well as the well-known CUF (with new non-polynomial shear strain shape function as in Refs. [11–13]) call the attention of new non-polynomial shear strain shape functions, which can be also included to this generalized HSDT for further evaluation.

In the present paper, a 5-unknowns generalized formulation with stretching effect for the bending analysis of functionally graded plates is presented for the first time. Infinite quasi-3D hybrid type (polynomial, non-polynomial, and hybrid) HSDTs, including the thickness expansion can be derived by using the present generalized theory. A free even transverse shear strain shape function, $g(z)$, for the proper distribution of the transverse shear strains through the plate thickness, can be utilized. The generalized theory complies with the tangential stress-free boundary conditions on the plate boundary surface, and thus a shear correction factor is not required. The plate governing equations and its boundary conditions are derived by employing the principle of virtual works. Navier-type analytical solution is obtained for plates subjected to transverse load for simply supported boundary conditions. Referential results for the displacement and stresses of functionally graded rectangular plates are obtained. The results are compared with 3D exact, quasi-exact, and with other closed-form solution published in the literature. Simple and accurate quasi-3D non-polynomial and hybrid HSDTs for bending analysis of FGPs were proposed for the first time.

2. Theoretical formulation

Fig. 1a shows a rectangular plate made of FGM of uniform thickness, h. The displacement field satisfying the free surfaces boundary conditions of transverse shear stresses (and hence strains) vanishing at a point $(x, y, \pm h/2)$ on the outer (top) and inner (bottom) surfaces of the plate, is given as follows:

$$\begin{aligned}
\overline{u} &= u + z\left[y^{**}\frac{\partial w_s}{\partial x} + q^{*}\frac{\partial \theta}{\partial x} - \frac{\partial w_b}{\partial x}\right] + f(z)\frac{\partial w_s}{\partial x},\\
\overline{v} &= v + z\left[y^{**}\frac{\partial w_s}{\partial y} + q^{*}\frac{\partial \theta}{\partial y} - \frac{\partial w_b}{\partial y}\right] + f(z)\frac{\partial w_s}{\partial y},\\
\overline{w} &= w_s + w_b + g(z)\theta,
\end{aligned} \tag{1a-c}$$

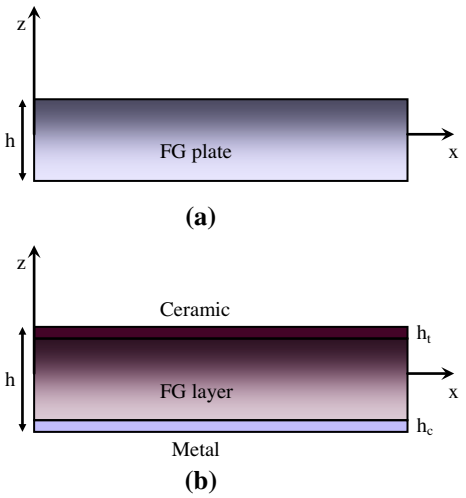

Fig. 1. Geometry of a functionally graded plate and sandwich plate.

where $u(x, y)$, $v(x, y)$, $w_s(x, y)$, $w_b(x, y)$ and $\theta(x, y)$ are the five unknown displacement functions of the middle surface of the panel, whilst for example in the case of the well known TPT $y^{**} = y^* - 1$, $y^* = 0$ and $q^* = 0$ (being h the thickness of the plate, see Table 1 for more details). The constants y^* and q^* are obtained by considering the criteria to reduce the number of unknowns in HSDTs as in Reddy and Liu [45]. They are as a function of the shear strain shape functions, $f(z)$ and $g(z)$, i.e. $y^* = -f'(h/2)$ and $q^* = -g(h/2)$.

For deriving the equations, small elastic deformations are assumed, i.e. displacements and rotations are small, and obey Hooke's law. The starting point of the present generalized quasi-3D hybrid type HSDT is the 3D elasticity theory [46]. The strain–displacement relations, based on this formulation, are written as follows:

$$\begin{aligned}
\varepsilon_{xx} &= \varepsilon^0_{xx} + z\varepsilon^1_{xx} + f(z)\varepsilon^2_{xx},\\
\varepsilon_{yy} &= \varepsilon^0_{yy} + z\varepsilon^1_{yy} + f(z)\varepsilon^2_{yy},\\
\varepsilon_{zz} &= g'(z)\varepsilon^5_{zz},\\
\varepsilon_{yz} &= \varepsilon^0_{yz} + g(z)\varepsilon^3_{yz} + f'(z)\varepsilon^4_{yz},\\
\varepsilon_{xz} &= \varepsilon^0_{xz} + g(z)\varepsilon^3_{xz} + f'(z)\varepsilon^4_{xz},\\
\varepsilon_{xy} &= \varepsilon^0_{xy} + z\varepsilon^1_{xy} + f(z)\varepsilon^2_{xy},
\end{aligned} \tag{2a-f}$$

where

$$\begin{aligned}
&\varepsilon^0_{xx} = \tfrac{\partial u}{\partial x}, && \varepsilon^1_{xx} = y^{**}\tfrac{\partial^2 w_s}{\partial x^2} + q^*\tfrac{\partial^2 \theta}{\partial x^2} - \tfrac{\partial^2 w_b}{\partial x^2}, && \varepsilon^2_{xx} = \tfrac{\partial^2 w_s}{\partial x^2},\\
&\varepsilon^0_{yy} = \tfrac{\partial v}{\partial y}, && \varepsilon^1_{yy} = y^{**}\tfrac{\partial^2 w_s}{\partial y^2} + q^*\tfrac{\partial^2 \theta}{\partial y^2} - \tfrac{\partial^2 w_s}{\partial y^2}, && \varepsilon^2_{yy} = \tfrac{\partial^2 w_s}{\partial y^2},\\
&\varepsilon^5_{zz} = \theta,\\
&\varepsilon^0_{yz} = y^*\tfrac{\partial w_s}{\partial y} + q^*\tfrac{\partial \theta}{\partial y}, && \varepsilon^3_{yz} = \tfrac{\partial \theta}{\partial y}, && \varepsilon^4_{yz} = \tfrac{\partial w_s}{\partial y},\\
&\varepsilon^0_{xz} = y^*\tfrac{\partial w_s}{\partial x} + q^*\tfrac{\partial \theta}{\partial x}, && \varepsilon^3_{xz} = \tfrac{\partial \theta}{\partial x}, && \varepsilon^4_{xz} = \tfrac{\partial w_s}{\partial x},\\
&\varepsilon^0_{xy} = \tfrac{\partial v}{\partial x} + \tfrac{\partial u}{\partial y}, && \varepsilon^1_{xy} = 2y^{**}\tfrac{\partial^2 w_s}{\partial x \partial y} + 2q^*\tfrac{\partial^2 \theta}{\partial x \partial y} - 2\tfrac{\partial^2 w_b}{\partial x \partial y}, && \varepsilon^2_{xy} = 2\tfrac{\partial^2 w_s}{\partial x \partial y},
\end{aligned} \tag{3a-p}$$

Table 1
Shear strain shape functions.

Model	$f(z)$ and $g(z)$ function	Particularities
Present polynomial HSDT (HSDT1)	$f(z) = z^3$ $g(z) = z^2$	$y^* = -\frac{3}{4}h^2$ $q^* = -\frac{h^2}{4}$
Present trigonometric HSDT (HSDT2)	$f(z) = 4h\sin(\frac{z}{4h})$ $g(z) = \cos(\frac{z}{4h})$	$y^* = -\cos(\frac{1}{8})$ $q^* = -\cos(\frac{1}{8})$
Present trigonometric HSDT (HSDT3)	$f(z) = \tan(\frac{z}{5h})$ $g(z) = \cos(\frac{z}{4h})$	$y^* = -\frac{1}{5h}\sec^2(\frac{1}{10})$ $q^* = -\cos(\frac{1}{8})$
Present hybrid HSDT (HSDT4)[+]	$f(z) = ze^{mz^2}$ $g(z) = nz^2$	$q^* = -(1 - \frac{mh^2}{2})e^{mh^2/4}$, $q^* = -\frac{nh^2}{4}$
Present hybrid HSDT (HSDT5) [*]	$f(z) = mz^3$ $g(z) = e^{nz^2}$	$y^* = -\frac{3m}{4}h^2$ $q^* = -e^{nh^2/4}$

[+] $m = 1/h^2$, $n = 1$.
[*] $m = 1$, $n = 1/h^2$.

An FGP of length a, width b and a total thickness h made of a mixture of metal and ceramic materials are considered in the present analysis. The elastic material properties vary through the thickness and the power-law distribution is assumed to describe the variation of material properties, which is expressed as

$$P(z) = \begin{cases} VP_b, & V = e^{p(\frac{z}{h}+\frac{1}{2})}, \quad \text{for exponentially graded plates.} \\ (P_t - P_b)V + P_b, & V = (\frac{z}{h}+\frac{1}{2})^p, \quad \text{for functionally graded plates (mixture rule).} \end{cases}, \tag{4a-b}$$

where P denotes the effective material property, P_t and P_b denote the property of the top and bottom faces of the panel, respectively, and p is the power-law exponent that specifies the material variation profile through the thickness. Fig. 2 shows the exponential function ($V_{\bar{z}}$) along the thickness of an exponentially graded plate (EGP) for different values of the parameter p. While Fig. 3 shows the corresponding function for FGMs obeying the rule of mixture.

The effective material properties of the plate, including Young's modulus, E, and shear modulus, G, vary according to Eq. (4a-b), and Poisson ratio, v is assumed to be constant.

The linear constitutive relations are given below:

$$\begin{Bmatrix} \sigma_{xx} \\ \sigma_{yy} \\ \sigma_{zz} \\ \tau_{yz} \\ \tau_{xz} \\ \tau_{xy} \end{Bmatrix}_{(z)} = \begin{bmatrix} Q_{11} & Q_{12} & Q_{13} & 0 & 0 & 0 \\ Q_{21} & Q_{22} & Q_{23} & 0 & 0 & 0 \\ Q_{31} & Q_{32} & Q_{33} & 0 & 0 & 0 \\ 0 & 0 & 0 & Q_{44} & 0 & 0 \\ 0 & 0 & 0 & 0 & Q_{55} & \\ 0 & 0 & 0 & 0 & 0 & Q_{66} \end{bmatrix}_{(z)} \begin{Bmatrix} \varepsilon_{xx} \\ \varepsilon_{yy} \\ \varepsilon_{zz} \\ \gamma_{yz} \\ \gamma_{xz} \\ \gamma_{xy} \end{Bmatrix}_{(z)}, \tag{5}$$

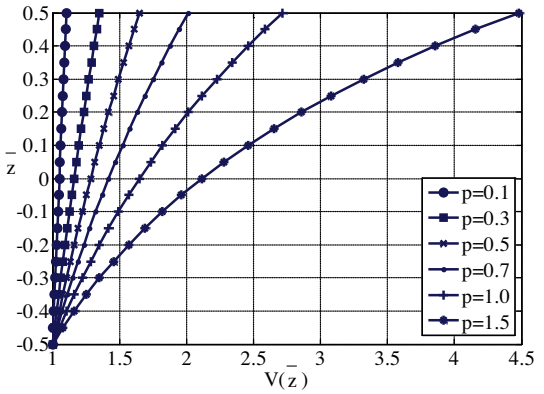

Fig. 2. Exponentially graded function $V(\bar{z})$ along the thickness of an EG plate for different values of the parameter "p".

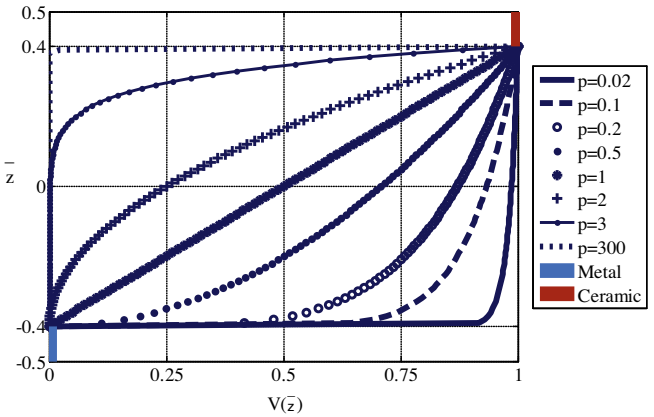

Fig. 3. Variations of non-dimensionalized vertical deflection with parameters "m" and "n" (HSDT1, $a/b = 1/6$, $a/h = 2$ and $p = 1.5$).

in which, $\sigma_{(z)} = \{\sigma_{xx}, \sigma_{yy}, \sigma_{zz}, \tau_{yz}, \tau_{xz}, \tau_{xy}\}^{T}$ and $\varepsilon_{(z)} = \{\varepsilon_{xx}, \varepsilon_{yy}, \varepsilon_{zz}, \gamma_{yz}, \gamma_{xz}, \gamma_{xy}\}^{T}$ are the stresses and the strain vectors with respect to the plate coordinate system. The Q_{ij} expressions in terms of engineering constants are given below:

$$Q_{11(z)} = Q_{22(z)} = Q_{33(z)} = \frac{E(z)(1-v)}{(1-2v)(1+v)},$$
$$Q_{12(z)} = Q_{13(z)} = Q_{23(z)} = \frac{E(z)v}{(1-2v)(1+v)}, \tag{6a-c}$$
$$Q_{44(z)} = Q_{55(z)} = Q_{66(z)} = \frac{E(z)}{2(1+v)}.$$

The modulus E, G and the elastic coefficients Q_{ij} vary through the thickness according to Eq. (4a-b), i.e. they are functions of z coordinate (depending on vertical position).

Considering the static version of the principle of virtual works, the following expressions can be obtained:

$$0 = \left[\int_{-h/2}^{h/2}\left\{\int_{\Omega}[\sigma_{xx}\delta\varepsilon_{xx} + \sigma_{yy}\delta\varepsilon_{yy} + \sigma_{zz}\delta\varepsilon_{zz} + \sigma_{yz}\delta\varepsilon_{yz} + \sigma_{xz}\delta\varepsilon_{xz} + \sigma_{xy}\delta\varepsilon_{xy}]dxdy\right\}dz\right] - \left[\int_{\Omega} q\delta\overline{w}dxdy\right], \tag{7}$$

$$\begin{aligned} 0 = \int_{\Omega}(&N_1\delta\varepsilon^0_{xx} + M_1\delta\varepsilon^1_{xx} + P_1\delta\varepsilon^2_{xx} + N_2\delta\varepsilon^0_{yy} + M_2\delta\varepsilon^1_{yy} + P_2\delta\varepsilon^2_{yy} + R_3\delta\varepsilon^4_{zz} + N_4\delta\varepsilon^0_{yz} + Q_4\delta\varepsilon^3_{yz} + K_4\delta\varepsilon^4_{yz} + N_5\delta\varepsilon^0_{xz} \\ &+ Q_5\delta\varepsilon^3_{xz} + K_5\delta\varepsilon^4_{xz} + N_6\delta\varepsilon^0_{xy} + M_6\delta\varepsilon^1_{xy} + P_6\delta\varepsilon^2_{xy} - q\delta\overline{w})dxdy, \end{aligned} \tag{8}$$

where ε or σ are the stresses and the strain vectors, q is the distributed transverse load; and N_i, M_i, P_i, Q_i, K_i and R_i are the resultants of the following integrations:

$$\begin{aligned} &(N_i, M_i, P_i) = \int \sigma_{i(z)}(1, z, f(z))dz, \quad (i = 1, 2, 6), \\ &N_i = \int \sigma_{i(z)}dz, \quad (i = 4, 5), \\ &(Q_i, K_i) = \sum_{k=1}^{N}\int_{z}^{z} \sigma_{i(z)}(g(z), f'(z))dz, \quad (i = 4, 5), \\ &R_i = \int \sigma^{(k)}_{i(z)}g'(z)dz. \quad (i = 3). \end{aligned} \tag{9a-d}$$

From Eq. (8), the generalized static version of the governing equations can be derived by integrating the displacement gradients by parts and setting the coefficients of δu, δv, δw_s, δw_b, and $\delta\theta$ to zero separately. The generalized bending equations obtained are as follows:

$$\begin{aligned} &\delta u : \frac{\partial N_1}{\partial x} + \frac{\partial N_6}{\partial y} = 0, \\ &\delta v : \frac{\partial N_2}{\partial y} + \frac{\partial N_6}{\partial x} = 0, \\ &\delta w_s : y^{**}\left(\frac{\partial^2 M_1}{\partial x^2} + \frac{\partial^2 M_2}{\partial y^2} + 2\frac{\partial^2 M_6}{\partial x\partial y}\right) - y^{*}\left(\frac{\partial N_5}{\partial x} + \frac{\partial N_4}{\partial y}\right) + \frac{\partial^2 P_1}{\partial x^2} + \frac{\partial^2 P_2}{\partial y^2} + 2\frac{\partial^2 P_6}{\partial x\partial y} - \frac{\partial K_5}{\partial x} - \frac{\partial K_4}{\partial y} = q, \\ &\delta w_b : -\frac{\partial^2 M_1}{\partial x^2} - \frac{\partial^2 M_2}{\partial y^2} - 2\frac{\partial^2 M_6}{\partial x\partial y} = q, \\ &\delta\theta : q^{*}\left(\frac{\partial^2 M_1}{\partial x_1^2} + \frac{\partial^2 M_2}{\partial x_2^2} + 2\frac{\partial^2 M_6}{\partial x_1\partial x_2} - \frac{\partial N_4}{\partial x_2} - \frac{\partial N_5}{\partial x_1}\right) - \frac{\partial Q_4}{\partial x_2} - \frac{\partial Q_5}{\partial x_1} - R_3 = -q^{*}q. \end{aligned} \tag{10a-e}$$

By substituting the stress–strain relations into the definitions of force and moment resultants (Eq. (9a-d)), the following constitutive equations are obtained:

$$
\begin{aligned}
N_i &= A_{ij}\varepsilon_j^0 + B_{ij}\varepsilon_j^1 + C_{ij}\varepsilon_j^2 + D_{ij}\varepsilon_j^3 + E_{ij}\varepsilon_j^4 + F_{ij}\varepsilon_j^5, \quad (i=1,2,4,5,6;\, j=1,2,\ldots,6),\\
M_i &= B_{ij}\varepsilon_j^0 + G_{ij}\varepsilon_j^1 + H_{ij}\varepsilon_j^2 + I_{ij}\varepsilon_j^3 + J_{ij}\varepsilon_j^4 + K'_{ij}\varepsilon_j^5, \quad (i=1,2,6;\, j=1,2,\ldots,6),\\
P_i &= C_{ij}\varepsilon_j^0 + H_{ij}\varepsilon_j^1 + L_{ij}\varepsilon_j^2 + M'_{ij}\varepsilon_j^3 + N'_{ij}\varepsilon_j^4 + O_{ij}\varepsilon_j^5, \quad (i=1,2,6;\, j=1,2,\ldots,6),\\
Q_i &= D_{ij}\varepsilon_j^0 + I_{ij}\varepsilon_j^1 + M_{ij}\varepsilon_j^2 + P'_{ij}\varepsilon_j^3 + Q'_{ij}\varepsilon_j^4 + R'_{ij}\varepsilon_j^5, \quad (i=4,5;\, j=1,2,\ldots,6),\\
K_i &= E_{ij}\varepsilon_j^0 + J_{ij}\varepsilon_j^1 + N'_{ij}\varepsilon_j^2 + Q'_{ij}\varepsilon_j^3 + S_{ij}\varepsilon_j^4 + T_{ij}\varepsilon_j^5, \quad (i=4,5;\, j=1,2,\ldots,6),\\
R_i &= F_{ij}\varepsilon_j^0 + K'_{ij}\varepsilon_j^1 + O_{ij}\varepsilon_j^2 + R'_{ij}\varepsilon_j^3 + T_{ij}\varepsilon_j^4 + U_{ij}\varepsilon_j^5 \quad (i=3;\, j=1,2,\ldots,6),
\end{aligned}
\tag{11a-f}
$$

where

$$
\begin{aligned}
(A_{ij}, B_{ij}, C_{ij}, D_{ij}, E_{ij}, F_{ij}) &= \textstyle\int_{-h/2}^{h/2} Q_{ij(z)}(1, z, f(z), g(z), f'(z), g'(z))dz,\\
(G_{ij}, H_{ij}, I_{ij}, J_{ij}, K'_{ij}) &= \textstyle\int_{-h/2}^{h/2} Q_{ij(z)}(z^2, zf(z), zg(z), zf'(z), zg'(z))dz,\\
(L_{ij}, M'_{ij}, N'_{ij}, O_{ij}) &= \textstyle\int_{-h/2}^{h/2} Q_{ij(z)}(f^2(z), f(z)g(z), f(z)f'(z), f(z)g'(z))dz,\\
(P'_{ij}, Q'_{ij}, R'_{ij}) &= \textstyle\int_{-h/2}^{h/2} Q_{ij(z)}(g^2(z), g(z)f'(z), g(z)g'(z))dz,\\
(S_{ij}, T_{ij}) &= \textstyle\int_{-h/2}^{h/2} Q_{ij(z)}(f'^2(z), f'(z)g'(z))dz,\\
U_{ij} &= \textstyle\int_{-h/2}^{h/2} Q_{ij(z)}g'^2(z)dz.
\end{aligned}
\qquad (j=1,2,\ldots,6).
\tag{12a-f}
$$

In the expressions N_i, M_i, P_i, Q_i, K_i, and R_i, the variables depending on x and y are the strains, ε_j^b ($b = 0,\ldots,5$) (see Eq. (11a-f)). Therefore, the terms in each of the generalized bending governing equations of a plate (Eq. (10a-e)), for example $\frac{\partial^2 N_i}{\partial x^2}$, $\frac{\partial^2 M_i}{\partial x^2}$, can be obtained by using Eq. (11a-f) as follows.

First of all, closed-form solutions of PDEs (like Eq. (10a-e)) for general boundary conditions are difficult. Navier type solutions can be used to validate the present theory; however, more general boundary conditions as in Ref. [47] will require other solution strategies which are also available in the literature.

It should be also kept in mind that the strains (see also Eq. (11a-f)) are expressed as a function of the 5-unknowns, described in Eq. (1a-c). These unknowns are expressed as Fourier series (see Eqs. (13a-e) and (14)), i.e. Navier type solution, in order to: (a) comply with the simply supported (SS3) boundary conditions (see Eq. (15a-b)); and (b) solve the partial differential equations (PDEs) given in Eq. (10a-e).

$$
\begin{aligned}
u(x,y) &= \sum_{r=1}^{\infty}\sum_{s'=1}^{\infty} U_{rs'}\cos(\alpha x)\sin(\beta y), \quad 0 \leqslant x \leqslant a;\ 0 \leqslant y \leqslant b,\\
v(x,y) &= \sum_{r=1}^{\infty}\sum_{s'=1}^{\infty} V_{rs'}\sin(\alpha x)\cos(\beta y), \quad 0 \leqslant x \leqslant a;\ 0 \leqslant y \leqslant b,\\
w_b(x,y) &= \sum_{r=1}^{\infty}\sum_{s'=1}^{\infty} W^b_{rs'}\sin(\alpha x)\sin(\beta y), \quad 0 \leqslant x \leqslant a;\ 0 \leqslant y \leqslant b,\\
w_s(x,y) &= \sum_{r=1}^{\infty}\sum_{s'=1}^{\infty} W^s_{rs'}\sin(\alpha x)\sin(\beta y), \quad 0 \leqslant x \leqslant a;\ 0 \leqslant y \leqslant b,\\
\theta(x,y) &= \sum_{r=1}^{\infty}\sum_{s'=1}^{\infty} \Theta_{rs'}\sin(\alpha x)\sin(\beta y), \quad 0 \leqslant x \leqslant a;\ 0 \leqslant y \leqslant b,
\end{aligned}
\tag{13a-e}
$$

where

$$
\alpha = \frac{r\pi}{a}, \quad \beta = \frac{s'\pi}{b},
\tag{14}
$$

$$
\begin{aligned}
N_1 = M_1 = P_1 = v = w_b = w_s = \frac{\partial w_s}{\partial y} = \theta \text{ at } x = 0, a,\\
N_2 = M_2 = P_2 = u = w_b = w_s = \frac{\partial w_s}{\partial x} = \theta \text{ at } y = 0, b.
\end{aligned}
\tag{15a-b}
$$

Then, by using Eqs. (13a-e) and (11a-f) along with the terms in the PDEs (Eq. (10a-e)), Eq. (16) can be obtained. Note that the term $\frac{\partial^2 M_i}{\partial x^2}$ is important for Eq. (10c-e), but $\frac{\partial^2 N_i}{\partial x^2}$ is just presented for generalization; actually, it is not presented in any of the PDEs' terms.

$$\frac{\partial^2(N_i,M_i)}{\partial x^2}=(A_{ij},B_{ij})\left[\begin{bmatrix}\alpha^3&0&0&0&0\\0&\alpha^2\beta&0&0&0\\0&0&0&0&0\\0&0&-y^*\alpha^2\beta&0&-q^*\alpha^2\beta\\0&0&-y^*\alpha^3&0&-q^*\alpha^3\\-\alpha^2\beta&-\alpha^3&0&0&0\end{bmatrix}\begin{bmatrix}U_{rs'}\\V_{rs'}\\W^s_{rs'}\\W^b_{rs'}\\\Theta_{rs'}\end{bmatrix}^T\times\begin{Bmatrix}SS\\SS\\SS\\SC\\CS\\CC\end{Bmatrix}+(B_{ij},G_{ij})\begin{bmatrix}0&0&y^{**}\alpha^4&-\alpha^4&q^*\alpha^4\\0&0&y^{**}\alpha^2\beta^2&-\alpha^2\beta^2&q^*\alpha^2\beta^2\\0&0&0&0&0\\0&0&0&0&0\\0&0&0&0&0\\0&0&-y^{**}2\alpha^3\beta&+2\alpha^2\beta&-2q^*\alpha^3\beta\end{bmatrix}\begin{bmatrix}U_{rs'}\\V_{rs'}\\W^s_{rs'}\\W^b_{rs'}\\\Theta_{rs'}\end{bmatrix}^T\times\begin{Bmatrix}SS\\SS\\SS\\SC\\CS\\CC\end{Bmatrix}+(C_{ij},H_{ij})\begin{bmatrix}0&0&\alpha^4&0&0\\0&0&\alpha^2\beta^2&0&0\\0&0&0&0&0\\0&0&0&0&0\\0&0&-2\alpha^3\beta&0&0\\0&0&0&0&0\end{bmatrix}\begin{bmatrix}U_{rs'}\\V_{rs'}\\W^s_{rs'}\\W^b_{rs'}\\\Theta_{rs'}\end{bmatrix}^T\times\begin{Bmatrix}SS\\SS\\SS\\SC\\CS\\CC\end{Bmatrix}+(D_{ij},I_{ij})\begin{bmatrix}0&0&0&0&0\\0&0&0&0&0\\0&0&0&0&0\\0&0&0&0&-\alpha^2\beta\\0&0&0&0&-\alpha^3\\0&0&0&0&0\end{bmatrix}\begin{bmatrix}U_{rs'}\\V_{rs'}\\W^s_{rs'}\\W^b_{rs'}\\\Theta_{rs'}\end{bmatrix}^T\times\begin{Bmatrix}SS\\SS\\SS\\SC\\CS\\CC\end{Bmatrix}+(E_{ij},J_{ij})\begin{bmatrix}0&0&0&0&0\\0&0&0&0&0\\0&0&0&0&0\\0&0&-\alpha^2\beta&0&0\\0&0&-\alpha^3&0&0\\0&0&0&0&0\end{bmatrix}\begin{bmatrix}U_{rs'}\\V_{rs'}\\W^s_{rs'}\\W^b_{rs'}\\\Theta_{rs'}\end{bmatrix}^T\times\begin{Bmatrix}SS\\SS\\SS\\SC\\CS\\CC\end{Bmatrix}+(F_{ij},K'_{ij})\begin{bmatrix}0&0&0&0&0\\0&0&0&0&0\\0&0&0&0&-\alpha^2\\0&0&0&0&0\\0&0&0&0&0\\0&0&0&0&0\end{bmatrix}\begin{bmatrix}U_{rs'}\\V_{rs'}\\W^s_{rs'}\\W^b_{rs'}\\\Theta_{rs'}\end{bmatrix}^T\times\begin{Bmatrix}SS\\SS\\SS\\SC\\CS\\CC\end{Bmatrix}, \tag{16}$$

where $SS=\sin(\alpha x)\sin(\beta y)$, $SC=\sin(\alpha x)\cos(\beta y)$ and so for, and the elements of the 6×5 matrices are the coefficients obtained after taking the second derivation of the strains expression in the Eq. (11a-f).

The 6×5 matrices associated with $\frac{\partial^2 M_i}{\partial x^2}$ in Eq. (16) have the notation $\overline{M}^{2,b}_x$ ($b=0,\ldots,5$). The symbols used in $\overline{M}^{a,b}_v(a=2,$ $b\in\{0,1,\ldots,5\}$ and $v=x$ in the previous example) are as follow: the first upper and lower characters (a,v) indicate the ath derivative with respect to v (second derivative with respect to x, in the previous example), and the second upper character, b, indicates that the derivative is associates with the strain ε^b_j ($b=0,\ldots,5$). Thus, the expression $\frac{\partial^2(N_i,M_i)}{\partial x^2}$, can be obtained as:

$$\frac{\partial^2(N_i,M_i)}{\partial x^2}=((A_{ij},B_{ij})\overline{M}^{2,0}_x+(B_{ij},G_{ij})\overline{M}^{2,1}_x+(C_{ij},H_{ij})\overline{M}^{2,2}_x+(D_{ij},I_{ij})\overline{M}^{2,3}_x+(E_{ij},J_{ij})\overline{M}^{2,4}_x+(F_{ij},K'_{ij})\overline{M}^{2,5}_x)\sin(\alpha x)\sin(\beta y), \tag{17}$$

where, for example, $\overline{M}^{2,0}_x$ is:

$$\overline{M}^{2,0}_x=\begin{bmatrix}\alpha^3&0&0&0&0\\0&\alpha^2\beta&0&0&0\\0&0&0&0&0\\0&0&-y^*\alpha^2\beta&0&-q^*\alpha^2\beta\\0&0&-y^*\alpha^3&0&-q^*\alpha^3\\-\alpha^2\beta&-\alpha^3&0&0&0\end{bmatrix}. \tag{18}$$

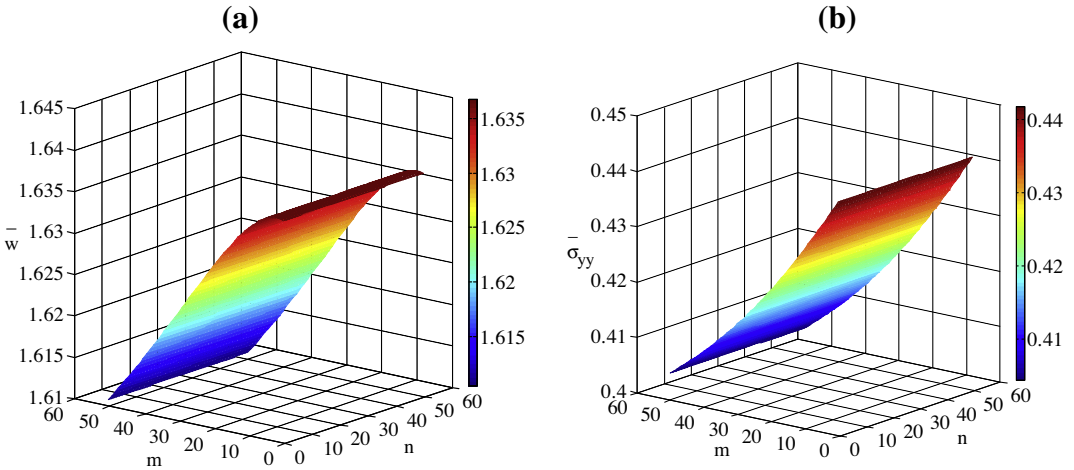

Fig. 4. Variations of non-dimensionalized inplane normal stresses with parameters "m" and "n" (HSDT1, $a/b=1/6$, $a/h=2$ and $p=1.5$).

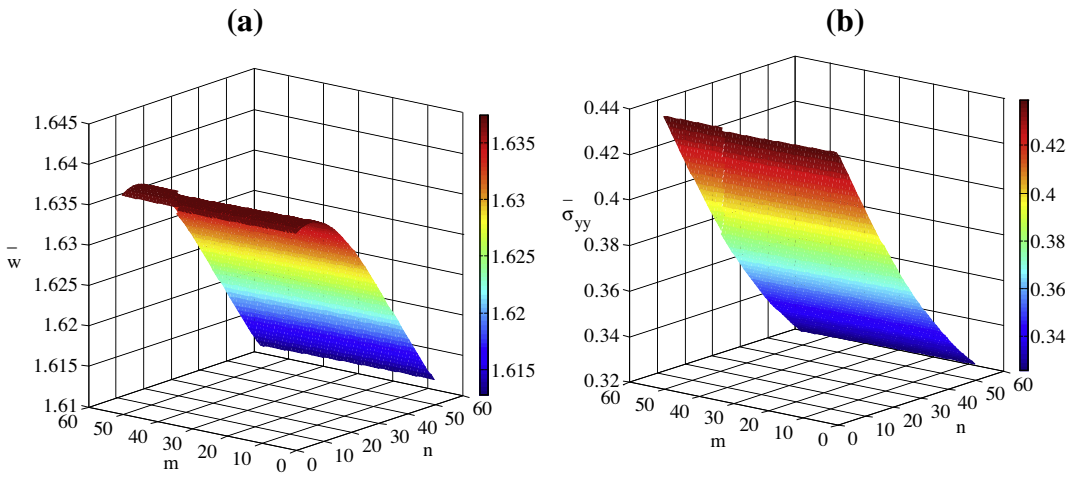

Fig. 5. Distribution of non-dimensionalized displacement, $\overline{w}$ ($a/2$, $b/2$, z), through the thickness of a thick ($a/h = 4$) EGP ($n = 0.5$).

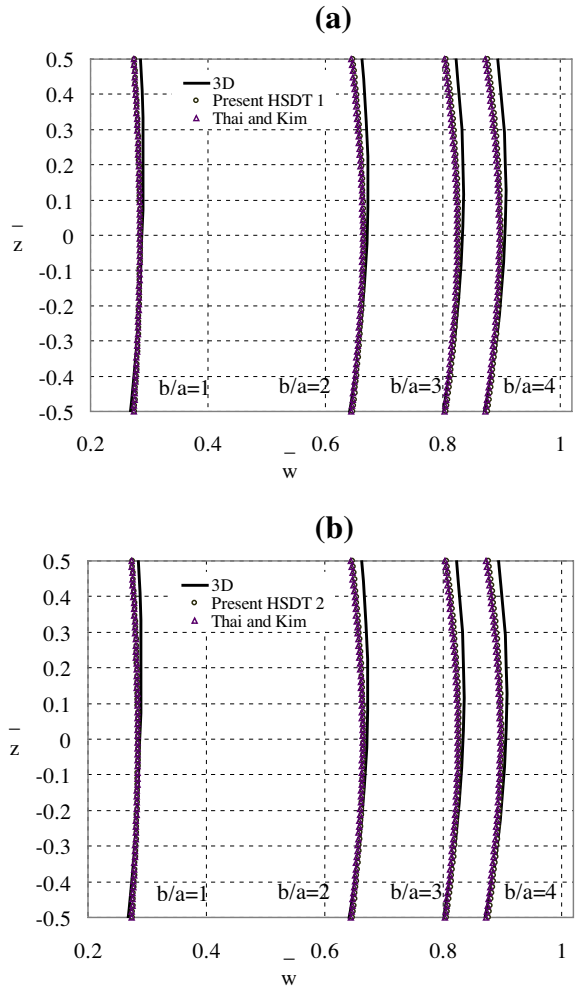

Fig. 6. Distribution of non-dimensionalized normal stress, $\overline{\sigma}_{xx}$ ($a/2$, $b/2$, z), through the thickness of a thick ($a/h = 4$) EGP ($n = 0.5$).

The matrices $\overline{M}_{\nu}^{a,b}$, associated with the expressions of the generalized bending governing equations (10a-e), for example $\frac{\partial M_i}{\partial x}$ or $\frac{\partial M_i}{\partial y}$, are given in the Appendix A.

3. Solution procedure

By substituting the potential solutions (Eq. (13a-e)) into the generalized bending governing equations (Eq. (10a-e)), the following linear equations are obtained,

$$K_{ij}d_j = F_j \quad (i,j = 1,\ldots,5) \quad and \quad (K_{ij} = K_{ji}). \tag{19}$$

For better understanding of the linear Eq. (19), the formulation of the first row of the stiffness matrix K_{ij} of Eq. (19) is described in detail. First of all, notice that it is built up considering the terms $\frac{\partial N_1}{\partial x}$ and $\frac{\partial N_6}{\partial y}$ (see Eq. (10a)). This equation can be expressed as follows:

$$\begin{aligned}\frac{\partial N_1}{\partial x} &= (A_{1j}\overline{M}_x^{1,0} + B_{1j}\overline{M}_x^{1,1} + C_{1j}\overline{M}_x^{1,2} + D_{1j}\overline{M}_x^{1,3} + E_{1j}\overline{M}_x^{1,4} + F_{1j}\overline{M}_x^{1,5})\sin(\alpha x)\sin(\beta y),\\ \frac{\partial N_i}{\partial y} &= (A_{6j}\overline{M}_y^{1,0} + B_{6j}\overline{M}_y^{1,1} + C_{6j}\overline{M}_y^{1,2} + D_{6j}\overline{M}_y^{1,3} + E_{6j}\overline{M}_y^{1,4} + F_{6j}\overline{M}_y^{1,5})\sin(\alpha x)\sin(\beta y),\end{aligned} \tag{20a-b}$$

where all the matrices $\overline{M}_{\nu}^{a,b}$ related to Eq. (20a-b) is given in Annex A. Consequently, if the sum both terms is done, it will deliver a 1×5 vector multiplied by $\sin(\alpha x)\sin(\beta y)$, this last term will be cancel out because the right hand of Equation 10a is 0. By the same procedure, the elements of stiffness matrix K_{ij} in Eq. (19) can be obtained. Note that:

$$\begin{aligned}\{d_j\}^T &= \{\, U'_{rs} \quad V_{rs'} \quad W^b_{rs'} \quad W^s_{rs'} \quad \Theta_{rs'} \,\},\\ \{F_j\}^T &= \{\, 0 \quad 0 \quad Q_{rs'} \quad Q_{rs'} \quad -q^* Q_{rs'} \,\},\end{aligned} \tag{21a-b}$$

where $Q_{rs'}$ are the coefficients in the double Fourier expansion of the transverse load,

$$q(x,y) = \sum_{r=1}^{\infty}\sum_{s'=1}^{\infty} Q_{rs'}\sin(\alpha x)\sin(\beta y). \tag{22}$$

Table 2
Non-dimensionalized centre deflection $\overline{w}$ $(a/2, b/2, 0)$ for various EGM rectangular plates, $a/h = \{2, 4\}$ (in bold the 3-D reference values).

a/h	b/a	Theory	$n = 0.1$	Diff.	$n = 0.3$	Diff.	$n = 0.5$	Diff.	$n = 0.7$	Diff.	$n = 1.0$	Diff.	$n = 1.5$	Diff.	Avrg.
2	6	3-D [42]	**1.63774**	**(%)**	**1.48846**	**(%)**	**1.35184**	**(%)**	**1.22688**	**(%)**	**1.05929**	**(%)**	**0.82606**	**(%)**	**(%)**
		Present HSDT1	1.6363	−0.1	1.4793	−0.6	1.3363	−1.2	1.2060	−1.7	1.0324	−2.5	0.7937	−3.9	1.7
		Present HSDT2	1.6363	−0.1	1.4793	−0.6	1.3362	−1.2	1.2060	−1.7	1.0325	−2.5	0.7937	−3.9	1.7
		Present HSDT3	1.6363	−0.1	1.4793	−0.6	1.3363	−1.2	1.2060	−1.7	1.0360	−2.2	0.7788	−5.7	1.9
		Present HSDT4	1.6368	−0.1	1.4797	−0.6	1.3366	−1.1	1.2062	−1.7	1.0325	−2.5	0.7935	−3.9	1.7
		Present HSDT5	1.6373	0.0	1.4802	−0.6	1.3371	−1.1	1.2068	−1.6	1.0332	−2.5	0.7944	−3.8	1.6
		Thai and Kim [34]	1.6294	−0.5	1.4731	−1.0	1.3307	−1.6	1.2010	−2.1	1.0282	−2.9	0.7906	−4.3	2.1
		TPT [42]	1.6294	−0.5	1.4731	−1.0	1.3307	−1.6	1.2010	−2.1	1.0282	−2.9	0.7906	−4.3	2.1
	1	3-D [42]	**0.57693**		**0.52473**		**0.47664**		**0.43240**		**0.37269**		**0.28904**		
		Present HSDT1	0.5776	0.1	0.5222	−0.5	0.4716	−1.1	0.4255	−1.6	0.3640	−2.3	0.2792	−3.4	1.5
		Present HSDT2	0.5776	0.1	0.5221	−0.5	0.4716	−1.1	0.4255	−1.6	0.3640	−2.3	0.2793	−3.4	1.5
		Present HSDT3	0.5777	0.1	0.5222	−0.5	0.4716	−1.1	0.4255	−1.6	0.3677	−1.3	0.2650	−8.3	2.2
		Present HSDT4	0.5784	0.3	0.5229	−0.4	0.4722	−0.9	0.4260	−1.5	0.3644	−2.2	0.2794	−3.3	1.4
		Present HSDT5	0.5790	0.4	0.5234	−0.2	0.4727	−0.8	0.4265	−1.4	0.3649	−2.1	0.2800	−3.1	1.3
		Thai and Kim [34]	0.5731	−0.7	0.5181	−1.3	0.4679	−1.8	0.4222	−2.4	0.3612	−3.1	0.2771	−4.1	2.2
		TPT [42]	0.5731	−0.7	0.5181	−1.3	0.4679	−1.8	0.4222	−2.4	0.3612	−3.1	0.2771	−4.1	2.2
4	6	3-D [42]	**1.17140**		**1.06218**		**0.96331**		**0.87378**		**0.75501**		**0.59193**		
		Present HSDT1	1.1703	−0.1	1.0582	−0.4	0.9563	−0.7	0.8636	−1.2	0.7403	−1.9	0.5713	−3.5	1.3
		Present HSDT2	1.1703	−0.1	1.0582	−0.4	0.9563	−0.7	0.8636	−1.2	0.7403	−1.9	0.5713	−3.5	1.3
		Present HSDT3	1.1703	−0.1	1.0582	−0.4	0.9563	−0.7	0.8636	−1.2	0.7403	−1.9	0.5713	−3.5	1.3
		Present HSDT4	1.1702	−0.1	1.0582	−0.4	0.9562	−0.7	0.8635	−1.2	0.7402	−2.0	0.5711	−3.5	1.3
		Present HSDT5	1.1696	−0.2	1.0576	−0.4	0.9557	−0.8	0.8631	−1.2	0.7400	−2.0	0.5711	−3.5	1.4
		Thai and Kim [34]	1.1668	−0.4	1.0551	−0.7	0.9534	−1.0	0.8611	−1.5	0.7382	−2.2	0.5697	−3.8	1.6
		TPT [42]	1.1668	−0.4	1.0551	−0.7	0.9535	−1.0	0.8611	−1.5	0.7382	−2.2	0.5697	−3.8	1.6
	1	3-D [42]	**0.34900**		**0.31677**		**0.28747**		**0.26083**		**0.22534**		**0.18054**		
		Present HSDT1	0.3486	−0.1	0.3152	−0.5	0.2848	−0.9	0.2571	−1.4	0.2203	−2.2	0.1697	−6.0	1.9
		Present HSDT2	0.3486	−0.1	0.3152	−0.5	0.2848	−0.9	0.2571	−1.4	0.2203	−2.2	0.1697	−6.0	1.9
		Present HSDT3	0.3486	−0.1	0.3152	−0.5	0.2848	−0.9	0.2571	−1.4	0.2203	−2.2	0.1697	−6.0	1.9
		Present HSDT4	0.3486	−0.1	0.3152	−0.5	0.2847	−1.0	0.2571	−1.4	0.2202	−2.3	0.1697	−6.0	1.9
		Present HSDT5	0.3485	−0.1	0.3151	−0.5	0.2847	−1.0	0.2570	−1.5	0.2202	−2.3	0.1697	−6.0	1.9
		Thai and Kim [34]	0.3475	−0.4	0.3142	−0.8	0.2839	−1.2	0.2563	−1.7	0.2196	−2.5	0.1692	−6.3	2.2
		TPT [42]	0.3475	−0.4	0.3142	−0.8	0.2839	−1.2	0.2563	−1.7	0.2196	−2.5	0.1692	−6.3	2.2

4. Numerical results and discussion

The results of the present generalized hybrid quasi-3D HSDT with 5-unknowns contemplates the recommendations regarding the stretching effect (see Ref. [10]). The target of this paper is present: (a) the mathematical formulation for the generalized hybrid quasi-3D HSDT with 5 unknowns; and (b) some new shear strain shape functions, which allows to produce polynomial, non-polynomial and quasi-3D hybrid type HSDTs.

It was not the intent of this paper to present the best quasi-3D HSDT having 5DOF. Future works may be conduced in order to find out the most accurate HSDT having a limited degree of freedom for classical and advanced composite plates. However, so far very accurate quasi-3D HSDT with 5 unknowns can be obtained by simply using referential shear strain shape functions developed previously by the authors [6–13,20–44,54–61,48] and some new ones presented in this paper for the first time (see Table 1).

Table 1 presents different couples of shear strain shape functions to be evaluated in the present generalized quasi-3D hybrid type HSDT with 5-unknowns. The first quasi-3D HSDT is a polynomial HSDT, the second HSDT is the well-known trigonometric quasi-3D HSDT, the third one is a new trigonometric quasi-3D HSDT, and the last two ones are of hybrid type (which combines polynomial with non-polynomial shape strain functions and vice versa, respectively), i.e. quasi-3D hybrid type HSDTs. For simplicity, the theories are called HSDT1, HSDT2 and so for (see Table 1).

In case of the present quasi-3D hybrid type HSDTs it is important to properly select the shears train function in order to get accurate results. However, for some hybrid shear strain functions such as exponential and trigonometric, this is not easy task. This is alleviated when one of the hybrid shears strain function is polynomial as in HSDT4 and HSDT5 (see Table 1). In this table, the shear strain shape function are expressed as a function of m and n, and by changing properly these parameters Figs. 4 and 5 can be plotted for HSDT4 and HSDT5, respectively. Regarding to m and n, it can be said that those are just

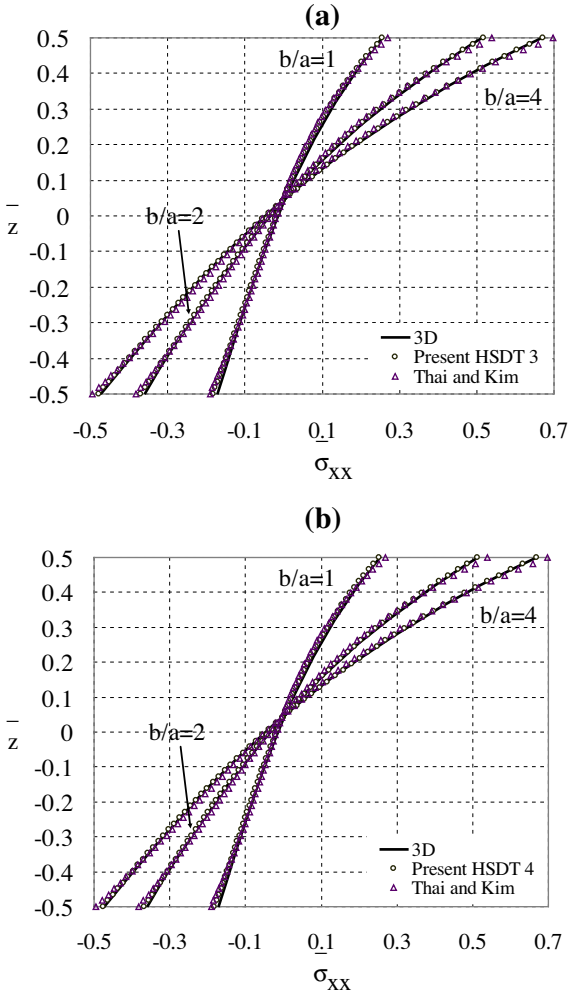

Fig. 7. Distribution of non-dimensionalized shear stress, $\overline{\sigma}_{xz}$ (0, $b/2$, z), through the thickness of a thick ($a/h = 4$) EGP ($n = 0.5$).

parameters of the shear strain shape functions to be properly selected in order to improve the accuracy of the solutions. Such parameters, in slightly different manner, are of paramount importance in 4-unknowns quasi-3D HSDTs as in Zenkour [49]. Figs. 4 and 5 show the nondimensionalized vertical displacement at ($a/2$, $b/2$, 0) (left side) and normal stresses at ($a/2$, $b/2$, $h/2$) (right side) as the function of the parameters m and n.

Note in Figs. 4 and 5 that the non-polynomial shear strain shape functions should be optimized to properly select the values of m for HSDT4 and n in this case of HSDT5, in order to get close to 3D results (readers may consult Refs. [48,50]). This is because polynomial shear strain functions ($g(z)$ in HSDT4 and $f(z)$ in the case of HSDT5) cannot be optimized following this idea, thus n and m does not have much influence in the results in Figs. 4 and 5, respectively (see HSDT4 and HSDT 5 in Table 1); ideas belonging to Matusanga [43], Xiang [51], Carrera et al. [10,52], Demasi [38] are good to produce accurate results in polynomial HSDTs. However, it is remarkable to mention the very recent work by Carrera et al. [40], where non-polynomial expansions of the in plane and transverse displacement were used by introducing non-polynomial series such as trigonometric ones. In this paper, $m = \frac{1}{h^2}$ (by optimization) and $n = 1$ (for simplicity) is considered for HSDT4; and $m = 1$ (for simplicity) and $n = \frac{1}{h^2}$ (by optimization) for HSDT5 considering in somehow the ideas belonging to Karama et al. [53].

4.1. Exponentially graded plates

The bending results of this example problem are compared with the 3D exact solutions and a HSDT with stretching effect by Zenkour [42]; a recently quasi-3D HSDT and 5 unknowns developed by Thai and Kim [34]; and the well-known trigonometric plate theory (quasi-3D TPT), which includes sinus function (Refs. [6,34,36,42,54–60]).

The FGM used in this section is composed by aluminum (bottom, Al), which is graded exponentially trough the thickness of a rectangular plate. The material properties used for computing the numerical results are:

$$E_b = 70\ \text{GPa}, \quad \nu_b = 0.3. \tag{23}$$

The following non-dimensional quantities are used:

$$\overline{w} = w\left(\frac{a}{2},\frac{b}{2},z\right)\frac{10E_b h^3}{q_0 a^4}, \quad \overline{\sigma}_{xx} = \sigma_{xx}\left(\frac{a}{2},\frac{b}{2},z\right)\frac{h^2}{q_0 a^2}, \quad \overline{\sigma}_{yy} = \sigma_{yy}\left(\frac{a}{2},\frac{b}{2},z\right)\frac{h^2}{q_0 a^2}, \quad \overline{\sigma}_{xz} = \sigma_{xz}\left(0,\frac{b}{2},z\right)\frac{h}{q_0 a}, \quad \overline{z} = \frac{z}{h}. \tag{24a-e}$$

Table 3
Nondimensionalized normal stresses $\overline{\sigma}_{yy}$ ($a/2$, $b/2$, $h/2$) for EGM rectangular plates, $a/h = \{2, 4\}$ (in bold the 3-D reference values).

a/h	b/a	Theory	$n = 0.1$	Diff.	$n = 0.3$	Diff.	$n = 0.5$	Diff.	$n = 0.7$	Diff.	$n = 1.0$	Diff.	$n = 1.5$	Diff.	Avrg.
2	6	3-D [42]	**0.2943**	(%)	**0.3101**	(%)	**0.3270**	(%)	**0.3451**	(%)	**0.3746**	(%)	**0.4305**	(%)	(%)
		Present HSDT1	0.2772	−5.8	0.2965	−4.4	0.3171	−3.0	0.3390	−1.8	0.3749	0.1	0.4433	3.0	3.0
		Present HSDT2	0.2773	−5.8	0.2966	−4.4	0.3171	−3.0	0.3391	−1.7	0.3750	0.1	0.4435	3.0	3.0
		Present HSDT3	0.2772	−5.8	0.2965	−4.4	0.3171	−3.0	0.3390	−1.8	0.3761	0.4	0.4351	1.1	2.7
		Present HSDT4	0.2751	−6.5	0.2942	−5.1	0.3145	−3.8	0.3363	−2.6	0.3717	−0.8	0.4394	2.1	3.5
		Present HSDT5	0.2706	−8.1	0.2892	−6.7	0.3091	−5.5	0.3304	−4.3	0.3652	−2.5	0.4318	0.3	4.6
		5DOF Quasi-3D [34]	0.2912	−1.0	0.3118	0.6	0.3339	2.1	0.3573	3.5	0.3955	5.6	0.4679	8.7	3.6
		TPT [42]	0.2912	−1.1	0.3118	0.6	0.3339	2.1	0.3573	3.5	0.3955	5.6	0.4679	8.7	3.6
	1	3-D [42]	**0.3103**		**0.3292**		**0.3495**		**0.3713**		**0.4068**		**0.4741**		
		Present HSDT1	0.2927	−5.7	0.3149	−4.3	0.3385	−3.1	0.3636	−2.1	0.4039	−0.7	0.4790	1.0	2.8
		Present HSDT2	0.2927	−5.7	0.3149	−4.3	0.3386	−3.1	0.3636	−2.1	0.4039	−0.7	0.4790	1.0	2.8
		Present HSDT3	0.2925	−5.7	0.3148	−4.4	0.3384	−3.2	0.3634	−2.1	0.4066	0.0	0.4611	−2.7	3.0
		Present HSDT4	0.2892	−6.8	0.3111	−5.5	0.3343	−4.4	0.3589	−3.3	0.3986	−2.0	0.4725	−0.3	3.7
		Present HSDT5	0.2928	−5.6	0.3151	−4.3	0.3387	−3.1	0.3637	−2.0	0.4039	−0.7	0.4787	1.0	2.8
		5DOF Quasi-3D [34]	0.2955	−4.8	0.3181	−3.4	0.3421	−2.1	0.3675	−1.0	0.4085	0.4	0.4851	2.3	2.3
		TPT [42]	0.2955	−4.8	0.3181	−3.4	0.3421	−2.1	0.3675	−1.0	0.4085	0.4	0.4851	2.3	2.3
4	6	3-D [42]	**0.2181**		**0.2321**		**0.2470**		**0.2628**		**0.2886**		**0.3373**		
		Present HSDT1	0.2141	−1.8	0.2271	−2.2	0.2411	−2.4	0.2563	−2.5	0.2817	−2.4	0.3319	−1.6	2.1
		Present HSDT2	0.2143	−1.8	0.2273	−2.1	0.2413	−2.3	0.2565	−2.4	0.2819	−2.3	0.3321	−1.5	2.1
		Present HSDT3	0.2143	−1.8	0.2272	−2.1	0.2413	−2.3	0.2565	−2.4	0.2818	−2.3	0.3320	−1.5	2.1
		Present HSDT4	0.2136	−2.1	0.2265	−2.4	0.2405	−2.6	0.2556	−2.7	0.2809	−2.7	0.3309	−1.9	2.4
		Present HSDT5	0.2021	−7.3	0.2139	−7.8	0.2268	−8.2	0.2408	−8.4	0.2644	−8.4	0.3119	−7.5	7.9
		5DOF Quasi-3D [34]	0.2369	8.6	0.2521	8.6	0.2683	8.6	0.2858	8.7	0.3144	9.0	0.3699	9.7	8.9
		TPT [42]	0.2369	8.6	0.2520	8.6	0.2683	8.6	0.2857	8.7	0.3144	9.0	0.3699	9.7	8.9
	1	3-D [42]	**0.2247**		**0.2400**		**0.2562**		**0.2736**		**0.3018**		**0.3589**		
		Present HSDT1	0.2244	−0.1	0.2398	−0.1	0.2563	0.0	0.2738	0.1	0.3024	0.2	0.3567	−0.6	0.2
		Present HSDT2	0.2245	−0.1	0.2399	0.0	0.2563	0.0	0.2739	0.1	0.3025	0.2	0.3568	−0.6	0.2
		Present HSDT3	0.2244	−0.1	0.2399	0.0	0.2563	0.0	0.2738	0.1	0.3024	0.2	0.3567	−0.6	0.2
		Present HSDT4	0.2236	−0.5	0.2389	−0.4	0.2552	−0.4	0.2727	−0.3	0.3011	−0.2	0.3551	−1.0	0.5
		Present HSDT5	0.2191	−2.5	0.2341	−2.5	0.2500	-2.4	0.2670	−2.4	0.2948	−2.3	0.3480	−3.0	2.5
		5DOF Quasi-3D [34]	0.2346	4.4	0.2510	4.6	0.2684	4.8	0.2870	4.9	0.3171	5.1	0.3739	4.2	4.7
		TPT [42]	0.2346	4.4	0.2510	4.6	0.2684	4.8	0.2870	4.9	0.3171	5.1	0.3739	4.2	4.7

Fig. 6 shows the nondimenzionalized distribution of vertical maximum deflection through the plate thickness ($b/a = \{1, 2, 3, 4\}$, $a/h = 4$, $p = 0.1$). HSDT1 and HSDT2 in Fig. 6a and b, respectively, are compared with the 3D elasticity solution and with the HSDT by Thai and Kim [34]. Both predict well the no constant distribution of the central deflection. However, the results for $\bar{z} > 0$ not fit well to the 3D one. It is perhaps because the load is applied at $\bar{z} = 0.5$, and a refined description of the displacement field is needed. Imaginary layerwise mathematical models as in Bricheto and Carrera [61] perhaps can be an option.

Considering Fig. 6, if one has to choose a HSDT to model the displacement field, for simplicity, the polynomial HSDT can be a really good choice. Table 2 present results of non-dimensionalized maximum plate deflection for $\bar{z} = 0$. Errors respect to the 3D elasticity solutions are computed by using the Eq. (25a-c).

$$\begin{aligned} &\text{Error}(\%) = \frac{\sum_{i=1}^{6} |E_i|}{6}, \\ &E_i = \frac{\overline{w}^p_{present} - \overline{w}^p_{exact}}{\overline{w}^p_{exact}} 100\%, \\ &p = \{0.1, 0.3, 0.5, 0.7, 1, 1.5\}. \end{aligned} \tag{25a-c}$$

Fig. 7 shows the nondimensionalized normal stresses, $\overline{\sigma}_{xx}$, through the plate thickness. HSDT3 and HSDT4 in Fig. 7a and b, respectively, are compared with 3D elasticity solution. Good results are achieved for both HSDTs. However, HSDT4 does not produce as good results as HSDT1, HSDT2 and HSDT3, see the normal stresses results, $\overline{\sigma}_{yy}$, in Table 3. In this table, also the results of the hybrid type (polynomial and exponential) HSDT5 is not accurate. It evidence that when exponential (hyperbolic) shear strain shape functions are used, the results are not always as expected.

Fig. 8 shows nondimensionalized shear stresses, $\overline{\sigma}_{xz}$, distribution through the plate thickness obtained from the five different quasi-3D HSDTs (see Fig. 8a–d). All these quasi-3D HSDTs produces good results compared with 3D solution and superior than the quasi-3D HSDT provided in Ref. [34]. Again, for simplicity, if one has to choose a quasi-3D HSDT, all point to the HSDT1.

Table 4
Nondimensionalized stress and deflection of sandwich square plates embedding an FG core with a polynomial material law.

p	Theory	$\overline{\sigma}_{xz}$ (0, $b/2$, $h/6$)			$\overline{w}$ ($a/2$, $b/2$, 0)		
		$a/h = 4$	$a/h = 10$	$a/h = 100$	$a/h = 4$	$a/h = 10$	$a/h = 100$
1	Present HSDT1	0.271	0.272	0.273	0.728	0.606	0.583
	Present HSDT2	0.271	0.272	0.273	0.728	0.606	0.583
	Present HSDT3	0.271	0.272	0.273	0.728	0.606	0.583
	Present HSDT4	0.270	0.271	0.271	0.728	0.606	0.583
	Present HSDT5	0.272	0.273	0.273	0.728	0.606	0.582
	Thai and Tim [34]	0.272	0.273	0.273	0.725	0.604	0.581
	Quasi-3D [12]	0.274	0.279	0.279	0.742	0.631	0.609
	Quasi-3D [62]	0.223	0.227	0.227	0.742	0.631	0.609
	Quasi-3D [63]	0.275	0.279	0.280	0.742	0.631	0.609
	Quasi-3D [10]	0.260	0.259	0.259	0.763	0.632	0.607
	FSDT [10]	0.246	0.246	0.246	0.774	0.634	0.607
4	Present HSDT1	0.260	0.261	0.261	1.016	0.782	0.737
	Present HSDT2	0.260	0.261	0.261	1.016	0.782	0.737
	Present HSDT3	0.259	0.261	0.261	1.016	0.781	0.737
	Present HSDT4	0.254	0.255	0.256	1.013	0.781	0.737
	Present HSDT5	0.260	0.261	0.261	1.017	0.782	0.737
	Thai and Tim [34]	0.265	0.266	0.267	1.017	0.780	0.734
	Quasi-3D [12]	0.272	0.278	0.279	1.039	0.820	0.778
	Quasi-3D [62]	0.315	0.322	0.323	1.035	0.820	0.779
	Quasi-3D [63]	0.270	0.275	0.275	1.037	0.820	0.778
	Quasi-3D [10]	0.240	0.240	0.240	1.093	0.831	0.780
	FSDT [10]	0.188	0.188	0.188	1.029	0.819	0.780
10	Present HSDT1	0.190	0.191	0.191	1.153	0.832	0.770
	Present HSDT2	0.190	0.191	0.191	1.153	0.832	0.770
	Present HSDT3	0.190	0.195	0.088	1.153	0.833	0.770
	Present HSDT4	0.185	0.186	0.187	1.147	0.831	0.770
	Present HSDT5	0.190	0.191	0.192	1.152	0.828	0.766
	Thai and Tim [34]	0.190	0.191	0.191	1.153	0.831	0.769
	Quasi-3D [12]	0.202	0.206	0.206	1.178	0.865	0.805
	Quasi-3D [62]	0.295	0.300	0.300	1.172	0.864	0.805
	Quasi-3D [63]	0.200	0.203	0.204	1.175	0.865	0.805
	Quasi-3D [10]	0.193	0.194	0.195	1.217	0.874	0.808
	FSDT [10]	0.123	0.123	0.123	1.111	0.856	0.808

4.2. Functionally graded sandwich plates

A FGM made of a FG core and two isotropic skins (metal and ceramic), i.e. a sandwich FG plate, as shown in Fig. 1b, is considered for further studies in this section. The bottom skin is metal with thickness $h_b = 0.1h$ and the top skin is ceramic with thickness $h_t = 0.1h$. The core ($h_c = 0.8h$) has a Young modulus varying in thickness direction according to rule of mixtures described in Eq. (4b), see also Fig. 3.

$$E_b = 70\ \text{GPa}, \quad E_t = 380\ \text{GPa}, \quad \nu_b = \nu_t = 0.3. \tag{24}$$

The following non-dimensional quantities are used:

$$\overline{w} = w\left(\frac{a}{2}, \frac{b}{2}, z\right)\frac{10E_b h^3}{q_0 a^4}, \quad \overline{\sigma}_{xz} = \sigma_{xz}\left(0, \frac{b}{2}, z\right)\frac{h}{q_0 a}. \tag{25}$$

The non-dimensional transverse displacement, $\overline{w}$, and transverse shear stress , $\overline{\sigma}_{xz}$, are presented in Table 4. The present results are compared with accurate quasi-3D HSDTs by Carrera et al. [10] and Neves et al. [12,62,63]. The results for displacement and stresses are in close agreement with refined quasi-3D solutions. In general, the results presented in this example problem are in good agreement with Refs. [10,12,34,63]. The HSDT4 has slightly different results than the rest of HSDTs. As mentioned above this HSDT has a hybrid displacement field model (exponential and polynomial) as in [62] (hyperbolic function can be expressed as exponential functions). This perhaps explain why in [62] (even when 91 mathematical layers were used to model the continuous variation of properties across the thickness direction) not accurate results as in [10,63] were achieved.

Finally, it can be concluded that the present theories are more effective in the case of exponentially graded plates than in functionally graded plates (graded by using the rule of mixture). Further studies should be carried out for other gradation such as Mori–Tanaka.

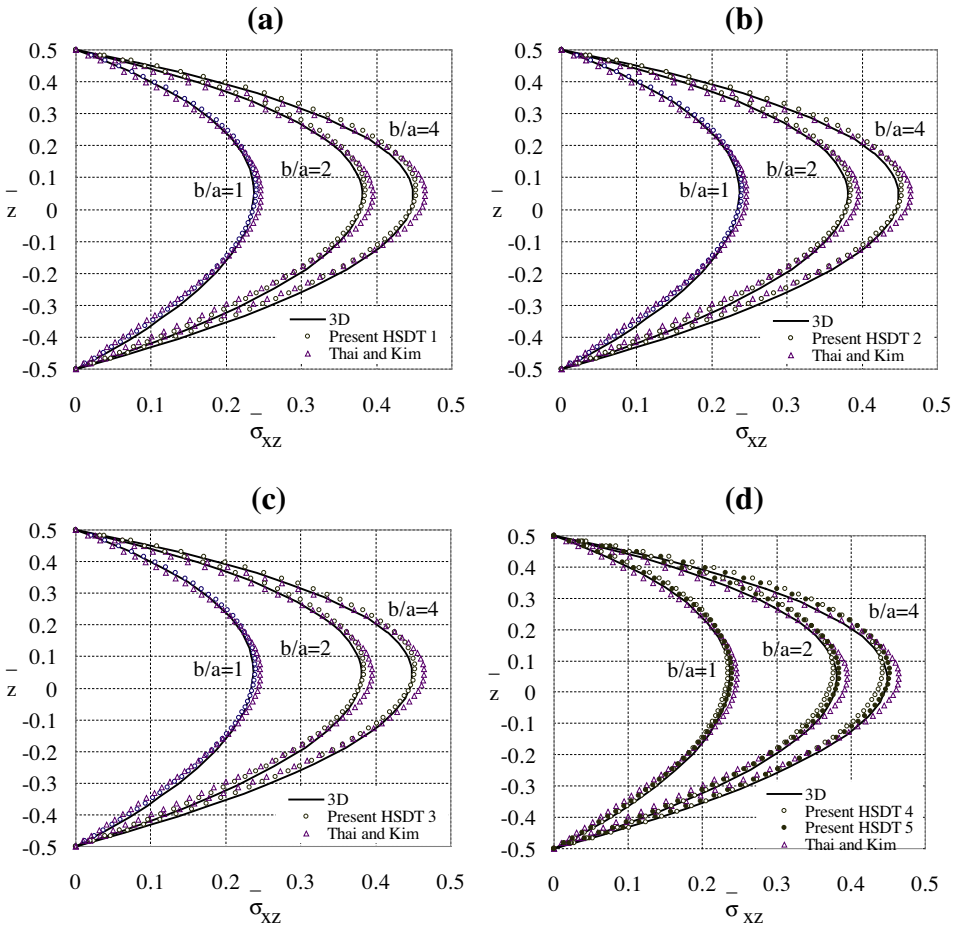

Fig. 8. Functionally graded function $V(\bar{z})$ along the thickness of an FG sandwich plate for different values of the parameter "p".

5. Conclusions

An unavailable generalized hybrid type quasi-3D HSDT with only 5-unknowns and stretching effects is presented in this paper. The governing equations and boundary conditions are derived by employing the principle of virtual works. A Navier-type closed-form solution is obtained for functionally graded single and sandwich plates subjected to bi-sinusoidal load for simply supported boundary conditions. Results show that the present TPT is capable to produce more accurate results than the FSDT, other HSDTs with higher number of unknowns. The important conclusions that emerge from this paper can be summarized as follows:

(a) Infinite shears strain shape function can be evaluated by using the present theory;
(b) So far polynomial shear strain functions are:
- easy to implement,
- simple to compute,
- and most important, in this type of quasi-3D HSDT produce very accurate results.
  Further studies need to be performed by using the infinite open possibilities to select shear strain shape function by the present generalized formulation.

(c) This generalized formulation with 5 unknowns and stretching effect can be as accurate as the 6-unknown generalized hybrid-type quasi-3D HSDT;
(d) The *best HSDT* with stretching effect and 5-unknows can be obtained from the present theory by using an optimizing procedure.

Acknowledgment

The first author wants to dedicate this paper to his friend Khoi Tran Nguyen who passed away pursuing his PhD degree. The first author has been financed by the Portuguese Foundation of Science and Technology under the contract number SFRH/BD/66847/2009.

Appendix A

Definition of matrices of type, $\overline{M}_v^{a,b}$

The matrices associated with the terms in the generalized bending governing equations (Eq. (10a-e)) are the following:

$$\overline{M}^{0,0}=\begin{bmatrix}-\alpha & 0 & 0 & 0 & 0\\ 0 & -\beta & 0 & 0 & 0\\ 0 & 0 & 0 & 0 & 0\\ 0 & 0 & y^*\beta & 0 & q^*\beta\\ 0 & 0 & y^*\alpha & 0 & q^*\alpha\\ \beta & \alpha & 0 & 0 & 0\end{bmatrix},\quad \overline{M}^{0,1}=\begin{bmatrix}0 & 0 & -y^{**}\alpha^2 & \alpha^2 & -q^*\alpha^2\\ 0 & 0 & -y^{**}\beta^2 & \beta^2 & -q^*\beta^2\\ 0 & 0 & 0 & 0 & 0\\ 0 & 0 & 0 & 0 & 0\\ 0 & 0 & 0 & 0 & 0\\ 0 & 0 & 2y^{**}\alpha\beta & -2\alpha\beta & 2q^*\alpha\beta\end{bmatrix},$$

$$\overline{M}^{0,2}=\begin{bmatrix}0 & 0 & -\alpha^2 & 0 & 0\\ 0 & 0 & -\beta^2 & 0 & 0\\ 0 & 0 & 0 & 0 & 0\\ 0 & 0 & 0 & 0 & 0\\ 0 & 0 & 0 & 0 & 0\\ 0 & 0 & 2\alpha\beta & 0 & 0\end{bmatrix},\quad \overline{M}^{0,3}=\begin{bmatrix}0 & 0 & 0 & 0 & 0\\ 0 & 0 & 0 & 0 & 0\\ 0 & 0 & 0 & 0 & 0\\ 0 & 0 & 0 & 0 & \beta\\ 0 & 0 & 0 & 0 & \alpha\\ 0 & 0 & 0 & 0 & 0\end{bmatrix},$$

$$\overline{M}^{0,4}=\begin{bmatrix}0 & 0 & 0 & 0 & 0\\ 0 & 0 & 0 & 0 & 0\\ 0 & 0 & 0 & 0 & 0\\ 0 & 0 & \beta & 0 & 0\\ 0 & 0 & \alpha & 0 & 0\\ 0 & 0 & 0 & 0 & 0\end{bmatrix},\quad \overline{M}^{0,5}=\begin{bmatrix}0 & 0 & 0 & 0 & 0\\ 0 & 0 & 0 & 0 & 0\\ 0 & 0 & 0 & 0 & 1\\ 0 & 0 & 0 & 0 & 0\\ 0 & 0 & 0 & 0 & 0\\ 0 & 0 & 0 & 0 & 0\end{bmatrix},$$

$$\overline{M}_x^{1,0} = \begin{bmatrix} -\alpha^2 & 0 & 0 & 0 & 0 \\ 0 & -\alpha\beta & 0 & 0 & 0 \\ 0 & 0 & 0 & 0 & 0 \\ 0 & 0 & y^*\alpha\beta & 0 & q^*\alpha\beta \\ 0 & 0 & -y^*\alpha^2 & 0 & -q^*\alpha^2 \\ -\alpha\beta & -\alpha^2 & 0 & 0 & 0 \end{bmatrix},$$

$$\overline{M}_x^{1,1} = \begin{bmatrix} 0 & 0 & -y^{**}\alpha^3 & \alpha^3 & -q^*\alpha^3 \\ 0 & 0 & -y^{**}\alpha\beta^2 & \alpha\beta^2 & -q^*\alpha\beta^2 \\ 0 & 0 & 0 & 0 & 0 \\ 0 & 0 & 0 & 0 & 0 \\ 0 & 0 & 0 & 0 & 0 \\ 0 & 0 & -2y^{**}\alpha^2\beta & 2\alpha^2\beta & -2q^*\alpha^2\beta \end{bmatrix},$$

$$\overline{M}_x^{1,2} = \begin{bmatrix} 0 & 0 & -\alpha^3 & 0 & 0 \\ 0 & 0 & -\alpha\beta^2 & 0 & 0 \\ 0 & 0 & 0 & 0 & 0 \\ 0 & 0 & 0 & 0 & 0 \\ 0 & 0 & 0 & 0 & 0 \\ 0 & 0 & -2\alpha^2\beta & 0 & 0 \end{bmatrix}, \quad \overline{M}_x^{1,3} = \begin{bmatrix} 0 & 0 & 0 & 0 & 0 \\ 0 & 0 & 0 & 0 & 0 \\ 0 & 0 & 0 & 0 & 0 \\ 0 & 0 & 0 & 0 & \alpha\beta \\ 0 & 0 & 0 & 0 & -\alpha^2 \\ 0 & 0 & 0 & 0 & 0 \end{bmatrix},$$

$$\overline{M}_x^{1,4} = \begin{bmatrix} 0 & 0 & 0 & 0 & 0 \\ 0 & 0 & 0 & 0 & 0 \\ 0 & 0 & 0 & 0 & 0 \\ 0 & 0 & \alpha\beta & 0 & 0 \\ 0 & 0 & -\alpha^2 & 0 & 0 \\ 0 & 0 & 0 & 0 & 0 \end{bmatrix}, \quad \overline{M}_x^{1,5} = \begin{bmatrix} 0 & 0 & 0 & 0 & 0 \\ 0 & 0 & 0 & 0 & 0 \\ 0 & 0 & 0 & 0 & \alpha \\ 0 & 0 & 0 & 0 & 0 \\ 0 & 0 & 0 & 0 & 0 \\ 0 & 0 & 0 & 0 & 0 \end{bmatrix},$$

$$\overline{M}_y^{1,0} = \begin{bmatrix} -\alpha\beta & 0 & 0 & 0 & 0 \\ 0 & -\beta^2 & 0 & 0 & 0 \\ 0 & 0 & 0 & 0 & 0 \\ 0 & 0 & -y^*\beta^2 & 0 & -q^*\beta^2 \\ 0 & 0 & y^*\alpha\beta & 0 & q^*\alpha\beta \\ -\beta^2 & -\alpha\beta & 0 & 0 & 0 \end{bmatrix}, \quad \overline{M}_y^{1,1} = \begin{bmatrix} 0 & 0 & -y^{**}\alpha^2\beta & \alpha^2\beta & -q^*\alpha^2\beta \\ 0 & 0 & -y^{**}\beta^3 & \beta^3 & -q^*\beta^3 \\ 0 & 0 & 0 & 0 & 0 \\ 0 & 0 & 0 & 0 & 0 \\ 0 & 0 & 0 & 0 & 0 \\ 0 & 0 & -2y^{**}\alpha\beta^2 & 2\alpha\beta^2 & -2q^*\alpha\beta^2 \end{bmatrix},$$

$$\overline{M}_y^{1,2} = \begin{bmatrix} 0 & 0 & -\alpha^2\beta & 0 & 0 \\ 0 & 0 & -\beta^3 & 0 & 0 \\ 0 & 0 & 0 & 0 & 0 \\ 0 & 0 & 0 & 0 & 0 \\ 0 & 0 & 0 & 0 & 0 \\ 0 & 0 & -2\alpha\beta^2 & 0 & 0 \end{bmatrix}, \quad \overline{M}_y^{1,3} = \begin{bmatrix} 0 & 0 & 0 & 0 & 0 \\ 0 & 0 & 0 & 0 & 0 \\ 0 & 0 & 0 & 0 & 0 \\ 0 & 0 & 0 & 0 & -\beta^2 \\ 0 & 0 & 0 & 0 & \alpha\beta \\ 0 & 0 & 0 & 0 & 0 \end{bmatrix},$$

$$\overline{M}_y^{1,4} = \begin{bmatrix} 0 & 0 & 0 & 0 & 0 \\ 0 & 0 & 0 & 0 & 0 \\ 0 & 0 & 0 & 0 & 0 \\ 0 & 0 & -\beta^2 & 0 & 0 \\ 0 & 0 & \alpha\beta & 0 & 0 \\ 0 & 0 & 0 & 0 & 0 \end{bmatrix}, \quad \overline{M}_y^{1,5} = \begin{bmatrix} 0 & 0 & 0 & 0 & 0 \\ 0 & 0 & 0 & 0 & 0 \\ 0 & 0 & 0 & 0 & \beta \\ 0 & 0 & 0 & 0 & 0 \\ 0 & 0 & 0 & 0 & 0 \\ 0 & 0 & 0 & 0 & 0 \end{bmatrix},$$

$$\overline{M}_y^{2,0} = \begin{bmatrix} \alpha\beta^2 & 0 & 0 & 0 & 0 \\ 0 & \beta^3 & 0 & 0 & 0 \\ 0 & 0 & 0 & 0 & 0 \\ 0 & 0 & -y^*\beta^3 & 0 & -q^*\beta^3 \\ 0 & 0 & -y^*\alpha\beta^2 & 0 & -q^*\alpha\beta^2 \\ -\beta^3 & -\alpha\beta^2 & 0 & 0 & 0 \end{bmatrix},$$

$$\overline{M}_y^{2,1} = \begin{bmatrix} 0 & 0 & y^{**}\alpha^2\beta^2 & -\alpha^2\beta^2 & q^*\alpha^2\beta^2 \\ 0 & 0 & y^{**}\beta^4 & -\beta^4 & q^*\beta^4 \\ 0 & 0 & 0 & 0 & 0 \\ 0 & 0 & 0 & 0 & 0 \\ 0 & 0 & 0 & 0 & 0 \\ 0 & 0 & -2y^{**}\alpha\beta^3 & \alpha\beta^3 & -2q^*\alpha\beta^3 \end{bmatrix},$$

$$\overline{M}_y^{2,2} = \begin{bmatrix} 0 & 0 & \alpha^2\beta^2 & 0 & 0 \\ 0 & 0 & \beta^4 & 0 & 0 \\ 0 & 0 & 0 & 0 & 0 \\ 0 & 0 & 0 & 0 & 0 \\ 0 & 0 & 0 & 0 & 0 \\ 0 & 0 & -2\alpha\beta^3 & 0 & 0 \end{bmatrix}, \quad \overline{M}_y^{2,3} = \begin{bmatrix} 0 & 0 & 0 & 0 & 0 \\ 0 & 0 & 0 & 0 & 0 \\ 0 & 0 & 0 & 0 & 0 \\ 0 & 0 & 0 & 0 & -\beta^3 \\ 0 & 0 & 0 & 0 & -\alpha\beta^2 \\ 0 & 0 & 0 & 0 & 0 \end{bmatrix},$$

$$\overline{M}_y^{2,4} = \begin{bmatrix} 0 & 0 & 0 & 0 & 0 \\ 0 & 0 & 0 & 0 & 0 \\ 0 & 0 & 0 & 0 & 0 \\ 0 & 0 & -\beta^3 & 0 & 0 \\ 0 & 0 & -\alpha\beta^2 & 0 & 0 \\ 0 & 0 & 0 & 0 & 0 \end{bmatrix}, \quad \overline{M}_y^{2,5} = \begin{bmatrix} 0 & 0 & 0 & 0 & 0 \\ 0 & 0 & 0 & 0 & 0 \\ 0 & 0 & 0 & 0 & -\beta^2 \\ 0 & 0 & 0 & 0 & 0 \\ 0 & 0 & 0 & 0 & 0 \\ 0 & 0 & 0 & 0 & 0 \end{bmatrix},$$

$$\overline{M}_{xy}^{2,0} = \begin{bmatrix} -\alpha^2\beta & 0 & 0 & 0 & 0 \\ 0 & -\alpha\beta^2 & 0 & 0 & 0 \\ 0 & 0 & 0 & 0 & 0 \\ 0 & 0 & -y^*\alpha\beta^2 & 0 & -q^*\alpha\beta^2 \\ 0 & 0 & -y^*\alpha^2\beta & 0 & -q^*\alpha^2\beta \\ \alpha\beta^2 & \alpha^2\beta & 0 & 0 & 0 \end{bmatrix},$$

$$\overline{M}_{xy}^{2,1} = \begin{bmatrix} 0 & 0 & -y^{**}\alpha^3\beta & \alpha^3\beta & -q^*\alpha^3\beta \\ 0 & 0 & -y^{**}\alpha\beta^3 & \alpha\beta^3 & -q^*\alpha\beta^3 \\ 0 & 0 & 0 & 0 & 0 \\ 0 & 0 & 0 & 0 & 0 \\ 0 & 0 & 0 & 0 & 0 \\ 0 & 0 & 2y^{**}\alpha^2\beta^2 & -2\alpha^2\beta^2 & 2q^*\alpha^2\beta^2 \end{bmatrix},$$

$$\overline{M}_{xy}^{2,2} = \begin{bmatrix} 0 & 0 & -\alpha^3\beta & 0 & 0 \\ 0 & 0 & -\alpha\beta^3 & 0 & 0 \\ 0 & 0 & 0 & 0 & 0 \\ 0 & 0 & 0 & 0 & 0 \\ 0 & 0 & 0 & 0 & 0 \\ 0 & 0 & 2\alpha^2\beta^2 & 0 & 0 \end{bmatrix}, \quad \overline{M}_{xy}^{2,3} = \begin{bmatrix} 0 & 0 & 0 & 0 & 0 \\ 0 & 0 & 0 & 0 & 0 \\ 0 & 0 & 0 & 0 & 0 \\ 0 & 0 & 0 & 0 & -\alpha\beta^2 \\ 0 & 0 & 0 & 0 & -\alpha^2\beta \\ 0 & 0 & 0 & 0 & 0 \end{bmatrix},$$

$$\overline{M}_{xy}^{2,4}=\begin{bmatrix}0&0&0&0&0\\0&0&0&0&0\\0&0&0&0&0\\0&0&-\alpha\beta^2&0&0\\0&0&-\alpha^2\beta&0&0\\0&0&0&0&0\end{bmatrix},\quad \overline{M}_{xy}^{2,5}=\begin{bmatrix}0&0&0&0&0\\0&0&0&0&0\\0&0&0&0&\alpha\beta\\0&0&0&0&0\\0&0&0&0&0\\0&0&0&0&0\end{bmatrix},$$

References

[1] M.B. Bever, P.E. Duwez, Gradients in composite materials, Mater. Sci. Eng. 10 (1972) 1–8.
[2] M. Koizumi, The concept of FGM, Ceram. Trans. Funct. Grad. Mater. 34 (1993) 3–10.
[3] V. Birman, L.W. Byrd, Modeling and analysis of functionally graded materials and structures, ASME Appl. Mech. Rev. 60 (2007) 195–216.
[4] J.L. Mantari, A.S. Oktem, C. Guedes Soares, Bending response of functionally graded plates by using a new higher order shear deformation theory, Compos. Struct. 94 (2012) 714–723.
[5] J.L. Mantari, C. Guedes Soares, Bending analysis of thick exponentially graded plates using a new trigonometric higher order shear deformation theory, Compos. Struct. 94 (2012) 1991–2000.
[6] J.L. Mantari, C. Guedes Soares, A novel higher-order shear deformation theory with stretching effect for functionally graded plates, Compos. B 45 (2013) 268–281.
[7] J.L. Mantari, C. Guedes Soares, Generalized hybrid quasi-3D shear deformation theory for the static analysis of advanced composite plates, Compos. Struct. 94 (2012) 2561–2575.
[8] J.L. Mantari, C. Guedes Soares, Finite element formulation of a generalized higher order shear deformation theory for advanced composite plates, Compos. Struct. 96 (2013) 545–553.
[9] D.K. Jha, R.K. Kant Tarun, A. Singh, A critical review of recent research on functionally graded plates, Compos. Struct. 96 (2013) 833–849.
[10] E. Carrera, S. Brischetto, M. Cinefra, M. Soave, Effects of thickness stretching in functionally graded plates and shells, Compos. B 42 (2011) 123–133.
[11] A.M.A. Neves, A.J.M. Ferreira, E. Carrera, C.M.C. Roque, M. Cinefra, R.M.N. Jorge, C.M.M. Soares, Bending of FGM plates by a sinusoidal plate formulation and collocation with radial basis functions, Mech. Res. Commun. 38 (2011) 368–371.
[12] A.M.A. Neves, A.J.M. Ferreira, E. Carrera, C.M.C. Roque, M. Cinefra, R.M.N. Jorge, C.M.M. Soares, A quasi-3D sinusoidal shear deformation theory for the static and free vibration analysis of functionally graded plates, Compos.: Part B: Eng. 43 (2) (2012) 711–725.
[13] A.J.M. Ferreira, E. Carrera, M. Cinefra, C.M.C. Roque, O. Polit, Analysis of laminated shells by a sinusoidal shear deformation theory and radial basis functions collocation, accounting for through-the-thickness deformations, Compos. B 42 (2011) 1276–1284.
[14] E. Carrera, M. Petrolo, Guidelines and recommendations to construct theories for metallic and composite plates, AIAA J. 48 (2010) 2852–2866.
[15] E. Carrera, M. Petrolo, On the effectiveness of higher-order terms in refined beam theories, J. Appl. Mech. 78 (2011).
[16] E. Carrera, F. Miglioretti, M. Petrolo, Guidelines and recommendations on the use of higher order finite elements for bending analysis of plates, Int. J. Comput. Methods Eng. Sci. Mech. 12 (6) (2011) 303–324.
[17] E. Carrera, F. Miglioretti, Selection of appropriate multilayered plate theories by using a genetic like algorithm, Compos. Struct. 94 (3) (2012) 1175–1186.
[18] E. Carrera, F. Miglioretti, Development of a best plate theories diagram for laminated plates including layer-wise and zigzag approaches, in: Hannover, 2011, pp. 21–23.
[19] E. Carrera, F. Miglioretti, Selection of appropriate plate theories by using a genetic like algorithms, in: 52nd AIAA/ASME/ASCE/AHS/ASC Structures, Structural Dynamics and Materials Conference. Denver, CO, (USA), 2011.
[20] J.L. Mantari, A.S. Oktem, C. Guedes Soares, A new trigonometric shear deformation theory for isotropic, laminated composite and sandwich plates, Int. J. Solids Struct. 49 (2012) 43–53.
[21] J.L. Mantari, A.S. Oktem, C. Guedes Soares, A new higher order shear deformation theory for sandwich and composite laminated plates, Compos. B 43 (2012) 1489–1499.
[22] J.L. Mantari, A.S. Oktem, C. Guedes Soares, A new trigonometric layerwise shear deformation theory for the finite element analysis of laminated composite and sandwich plates, Comput. Struct. 94–95 (2012) 45–53.
[23] J.L. Mantari, A.S. Oktem, C. Guedes Soares, Static and dynamic analysis of laminated composite and sandwich plates and shells by using a new higher-order shear deformation theory, Compos. Struct. 94 (2011) 37–49.
[24] J.L. Mantari, A.S. Oktem, C. Guedes Soares, Bending and free vibration analysis of isotropic and multilayered plates and shells by using a new accurate higher-order shear deformation theory, Compos. B 43 (2012) 3348–3360.
[25] J.L. Mantari, C. Guedes Soares, Analysis of isotropic and multilayered plates and shells by using a generalized higher-order shear deformation theory, Compos. Struct. 94 (2012) 2640–2656.
[26] R.P. Shimpi, Refined plate theory and its variants, AIAA J. 40 (1) (2002) 137–146.
[27] R.P. Shimpi, H.G. Patel, A two variable refined plate theory for orthotropic plate analysis, Int. J. Solids Struct. 43 (22) (2006) 6783–6799.
[28] R.P. Shimpi, H.G. Patel, Free vibrations of plate using two variable refined plate theory, J. Sound Vib. 296 (4–5) (2006) 979–999.
[29] I. Mechab, H. Ait Atmane, A. Tounsi, H.A. Belhadj, E.A. Adda Bedia, A two variable refined plate theory for bending of functionally graded plates, Acta Mech. Sin. 26 (6) (2010) 941.
[30] H.H. Abdelaziz, H.A. Atmane, I. Mechab, L. Boumia, A. Tounsi, A.B.E. Abbas, Static analysis of functionally graded sandwich plates using an efficient and simple refined theory, Chin. J. Aeronaut. 24 (2011) 434–448.
[31] M.S.A. Houari, S. Benyoucef, I. Mechab, A. Tounsi, E.A. Adda bedia, Two variable refined plate theory for thermoelastic bending analysis of functionally graded sandwich plates, J. Therm. Stresses 34 (2011) 315–334.
[32] A. Hamidi, M. Zidi, M.S.A. Houari, A. Tounsi, A new four variable refined plate theory for bending response of functionally graded sandwich plates under thermomechanical loading, Compos.: Part B (2012), http://dx.doi.org/10.1016/j.compositesb.2012.03.021.
[33] B. Mechab, I. Mechab, S. Benaissa, Static and dynamic analysis of functionally graded plates using four-variable refined plate theory by the new function, Compos. B 45 (2013) 748–757.
[34] H.T. Thai, S.E. Kim, A simple quasi-3D sinusoidal shear deformation theory for functionally graded plates, Compos. Struct. 99 (2013) 172–180.
[35] J.L. Mantari, C. Guedes Soares, A trigonometric plate theory with 5-unknows and stretching effect for advanced composite plates, Compos. Struct. 107 (2014) 396–405.
[36] K.P. Soldatos, A transverse shear deformation theory for homogeneous monoclinic plates, Acta Mech. 94 (1992) 195–220.
[37] E. Carrera, Theories and finite elements for multilayered plates and shells: a unified compact formulation with numerical assessment and benchmarks, Arch. Comput. Methods Eng. 10 (2003) 215–296.
[38] L. Demasi, ∞^3 Hierarchy plate theories for thick and thin composite plates: the generalized unified formulation, Compos. Struct. 84 (2008) 256–270.
[39] L. Demasi, ∞^6 Mixed plate theories based on the generalized unified formulation. Part I: governing equations, Compos. Struct. 87 (2009) 1–11.
[40] E. Carrera, M. Filippi, E. Zappino, Laminated beam analysis by polynomial, trigonometric, exponential and zig-zag theories, Euro. J. Mech. A/Solids 41 (2013) 58–69.

[41] A.M. Zenkour, Generalized shear deformation theory for bending analysis of functionally graded plates, Appl. Math. Model. 30 (2006) 67–84.
[42] A.M. Zenkour, Benchmark trigonometric and 3-D elasticity solutions for an exponentially graded thick rectangular plate, Appl. Math. Model. 77 (2007) 197–214.
[43] H. Matsunaga, Free vibration and stability of functionally graded plates according to 2-D higher-order deformation theory, Compos. Struct. 82 (2008) 256–270.
[44] Song Xiang, Gui-wen Kang, Static analysis of functionally graded plates by the various shear deformation theory, Compos. Struct. 99 (2013) 224–230.
[45] J.N. Reddy, C.F. Liu, A higher-order shear deformation theory of laminated elastic shells, Int. J. Eng. Sci. 23 (1985) 319–330.
[46] J.N. Reddy, Mechanics of Laminated Composite Plates: Theory and Analysis, 2nd ed., CRC Press, Boca Raton (FL), 2004.
[47] A.S. Oktem, J.L. Mantari, C. Guedes Soares, Static response of functionally graded plates and doubly-curved shells based on a higher order shear deformation theory, Euro. J. Mech. A/Solids 36 (2012) 163–172.
[48] J.L. Mantari, C. Guedes Soares, Optimized sinusoidal higher order shear deformation theory for the analysis of functionally graded plates and shells, Compos. B: Eng. 56 (2014) 126–136.
[49] A.M. Zenkour, A simple four-unknown refined theory for bending analysis of functionally graded plates, Appl. Math. Model. 37 (20–21) (2013) 9041–9051.
[50] J.L. Mantari, C. Guedes Soares, Four-unknown quasi-3D shear deformation theory for advanced composite plates, Compos. Struct. 109 (2014) 231–239.
[51] Song Xiang, Gui-wen Kang, A *n*th-order shear deformation theory for the bending analysis on the functionally graded plates, Euro. J. Mech. A/Solids 37 (2013) 336–343.
[52] E. Carrera, F. Miglioretti, M. Petrolo, Accuracy of refined elements for laminated plate analysis, Compos. Struct. 93 (2011) 1311–1327.
[53] M. Karama, K.S. Afaq, S. Mistou, Mechanical behavior of laminated composite beam by the new multilayered laminated composite structures model with transverse shear stress continuity, Int. J. Solid Struct. 40 (6) (2003) 1525–1546.
[54] M. Levy, Memoire sur la theorie des plaques elastique planes, J. Math. Pures Appl. 30 (1877) 219–306.
[55] M. Stein, Nonlinear theory for plates and shells including the effects of transverse shearing, AIAA 24 (9) (1986) 1537–1544.
[56] M. Touratier, An efficient standard plate theory, Int. J. Eng. Sci. 29 (8) (1991) 901–916.
[57] P. Vidal, O. Polit, A family of sinus finite elements for the analysis of rectangular laminated beams, Compos. Struct. 84 (2008) 56–72.
[58] P. Vidal, O. Polit, Assessment of the refined sinus model for the non-linear analysis of composite beams, Compos. Struct. 87 (2009) 370–381.
[59] P. Vidal, O. Polit, A sine finite element using a zig-zag function for the analysis of laminated composite beams, Compos. B 42 (2011) 1671–1682.
[60] P. Vidal, O. Polit, A refined sinus plate finite element for laminated and sandwich structures under mechanical and thermomechanical loads, Comput. Methods Appl. Mech. Eng. 253 (2013) 396–412.
[61] S. Brischetto, E. Carrera, Advanced mixed theories for bending analysis of functionally graded plates, Comput. Struct. 88 (2010) 1474–1483.
[62] A.M.A. Neves, A.J.M. Ferreira, E. Carrera, M. Cinefra, C.M.C. Roque, R.M.N. Jorge, A quasi-3D hyperbolic shear deformation theory for the static and free vibration analysis of functionally graded plates, Compos. Struct. 94 (5) (2012) 1814–1825.
[63] A.M.A. Neves, A.J.M. Ferreira, E. Carrera, M. Cinefra, C.M.C. Roque, R.M.N. Jorge, Static, free vibration and buckling analysis of isotropic and sandwich functionally graded plates using a quasi-3D higher-order shear deformation theory and a meshless technique, Compos. B: Eng. 44 (1) (2013) 657–674.